

# POLAR PLOTS OF DIAMOND SURFACE ENERGY

C.S. Bohun\*, J. Gravesen †, H. Laurie ‡, J. Hansen §

## Abstract

Diamond surface energy  $\sigma_{hkl}$  determines crystal habit. We discuss three aspects of a paper by Terentiev (1991). Firstly, we compare Terentiev's algorithm for exact  $\sigma_{hkl}$  with the analytic solution for  $h \leq k \leq l$  and  $h + k < l$ . Secondly, we show that the general formula given by Terentiev should be interpreted probabilistically in order to be self-consistent. Finally, we replicate in principle the simulation results for  $\sigma_{hkl}$  in a nickel melt using nothing more than Matlab routines.

## 1 Introduction

In this report, we investigate the surface energy of diamonds. The original motivation concerned the growth of industrial diamonds. Such diamonds may be grown from a solution of carbon in metal at relatively high temperature and pressure. At lower temperatures, the crystal habit tends to be cubic, and at higher temperatures it tends to be octahedral as illustrated in Figure 1. Since the cubic habit is more valuable in industrial diamonds, but the temperature range over which it forms is quite narrow, it seems desirable to develop a theoretical understanding of the role of temperature in the crystallisation of diamond from melt. The paper by Terentiev [1] discusses various aspects of this process. However, the presentation is in some

---

\*Department of Mathematics and Statistics, Pennsylvania State University, Pennsylvania, USA. *e-mail:* [csb15@psu.edu](mailto:csb15@psu.edu)

†Department of Mathematics, Technical University of Denmark, Denmark. *e-mail:* [j.gravesen@mat.dtu.dk](mailto:j.gravesen@mat.dtu.dk)

‡Department of Mathematics and Applied Mathematics, University of Cape Town, Rondebosch 7701, South Africa. *e-mail:* [henri.laurie@uct.ac.za](mailto:henri.laurie@uct.ac.za) and

§I.C. Consultants, PO Box 51190, Raedene 2124, Gauteng, South Africa. *e-mail:* [scrdochansen@gmail.com](mailto:scrdochansen@gmail.com)

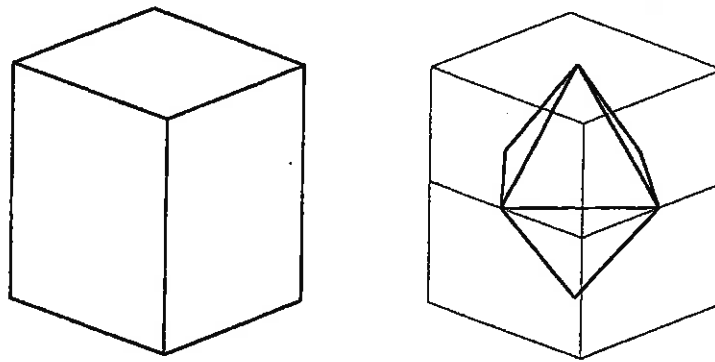


Figure 1: Two habits of diamond crystal. The octahedral habit is most common among natural diamonds, and cubic is most desired for industrial diamonds.

respects hard to follow and apparently contradictory. Our main aim in this report is to present Terentiev's results in a coherent and rigorous form.

We note that the paper by Terentiev [1] has not been much cited—we found only three entries in the ISI data base [2, 3, 4] and one in Google Scholar [5]. Following crystallographic convention, we denote by  $[hkl]$  the plane perpendicular to the vector  $\mathbf{n} = h\hat{\mathbf{i}} + k\hat{\mathbf{j}} + l\hat{\mathbf{k}}$ , and we use the standard unit cell of diamond with respect to these axes as shown in Figure 2. A given macrocrystal is composed of a very large number of unit cells. We consider only integer  $h$ ,  $k$  and  $l$ . Without loss of generality, we take  $h \leq k \leq l$  in lowest terms, that is, there is no integer which divides all three. The vacuum surface energy of the plane  $[hkl]$  is defined as the energy per unit area required to split the crystal into two along the plane. In other words, the energy per unit area of the bonds that cross the plane. All bonds in diamond are equivalent, so the vacuum surface energy is proportional to the number of bonds broken by the surface. For some orientations the position of the plane makes a difference to the number of bonds cut, and in those cases the real surface energy corresponds to the plane that breaks the fewest bonds. We use  $\sigma_{hkl}$  to denote the vacuum energy density of a diamond surface in the plane  $[hkl]$  in bonds per unit area, where the area of one face of the unit cube is 1.

In a melt, the surface energy is reduced as compared to a surface in a vacuum because the interaction between the crystal surface and the surrounding medium is equivalent to weak bonding. Hence in a melt the surface energy of a crystal is smaller than in vacuum. By definition, a melt is disordered and the position of atoms in the melt cannot be given by a regular pattern.

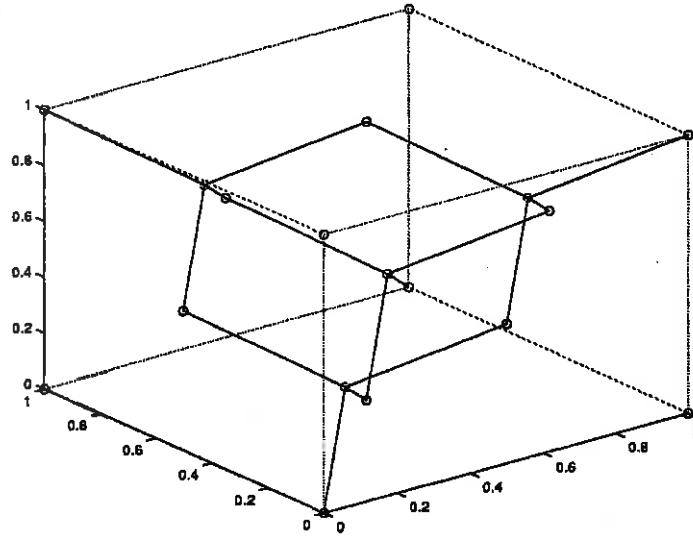


Figure 2: Unit cell of diamond lattice. It contains 18 atoms and 16 bonds. The bonds can be visualised by noting that four of the vertices do not form bonds internal to the unit cell, and that each of the four internal atoms bonds to one vertex and three face centres.

Terentiev [1] makes three contributions: a table of values for  $\sigma_{hkl}$  for several cases of small integers  $h$ ,  $k$  and  $l$ , reproduced as Table 1, the formula

$$\sigma_{hkl} = \sigma_{\{111\}} \sum_{i=1}^4 x_i \cos(\Phi_i), \quad (1)$$

(where the  $x_i$  and the  $\Phi_i$  depend on  $hkl$ —details are given in Equation (3)), and a diagram of  $\sigma_{hkl}$  versus temperature for two different surfaces in a melt based on a simulation driven by the joint potential of all the atoms in a melt. Accordingly, we structure this report around three related questions.

A: Terentiev used a computer search to find the entries in his table. Can one find an expression in closed form that gives the correct values?

B: If the answer to A is in the affirmative, how does Equation 3 relate to the  $\sigma_{hkl}$  in the table?

C: Can Terentiev's simulated temperature-dependence of  $\sigma_{hkl}$  for diamonds in a melt be replicated?

In Section 2, we discuss the first question. We formulate an equivalent minimisation problem and solve it for the case  $h+k < l$ . In Section 3 we show that Equation 3 leads to a contradiction if interpreted deterministically but holds when the left-hand side is interpreted probabilistically. In Section 4

Plane	Terentiev value	Formula 2
001	4.0004	4
<b>011</b>	2.8284	2.8284
012	3.5765	3.5777
111	2.3094	2.3904
<b>112</b>	3.2652	3.2660
113	3.6198	3.6181
023	3.3282	3.3084
<b>123</b>	3.0922	3.2071

Table 1: Diamond surface energies for various orientations of the surface. Energy is in number of bonds per unit area, where the edge length of a unit cell is 1. The first column gives  $hkl$ , where  $h \leq k \leq l$ ; bold face indicates  $h + k \geq l$ . The second column gives the values reported by Terentiev [1], rescaled to the current energy unit. The third column gives the value calculated according to the formula reported here. Note that although the formula was proved correct only for the case  $h + k < l$ , it matches the Terentiev value in some other cases.

we answer question C affirmatively and, thanks to Matlab, using only a few lines of code; we also consider other possible approaches to the simulation.

## 2 Analytical investigation of vacuum $\sigma_{hkl}$

When  $h$ ,  $k$  and  $l$  are integers, the intersection of the plane  $[hkl]$  with the diamond lattice forms a regular tessellation. The smallest unit parallelogram of this tessellation is formed by the vectors  $\mathbf{v} = -k\hat{\mathbf{i}} + h\hat{\mathbf{j}}$  and  $\mathbf{w} = -l\hat{\mathbf{i}} + h\hat{\mathbf{k}}$ . This is easily proved as follows. The plane is perpendicular to  $\mathbf{n} = h\hat{\mathbf{i}} + k\hat{\mathbf{j}} + l\hat{\mathbf{k}}$ , and since  $\mathbf{v}$  and  $\mathbf{w}$  are orthogonal to  $\mathbf{n}$ , they both lie in the plane  $[hkl]$ . Hence they define a parallelogram that tessellates the plane. To prove that it is the smallest of possible unit parallelograms, consider its area  $A_{hkl} = \|\mathbf{v} \times \mathbf{w}\|_2 = h\sqrt{h^2 + k^2 + l^2}$ . Any other unit parallelogram must also be formed by vectors with integer components chosen from  $h$ ,  $k$ ,  $l$  and their multiples, for otherwise two adjacent parallelograms would differ in the patterns formed by the bonds they cut. But because  $k$  and  $l$  cannot be smaller than  $h$ , the area of another unit parallelogram cannot be smaller than  $A_{hkl}$  which is therefore the smallest possible area of a tessellating parallelogram. Hence  $\mathbf{v}$  and  $\mathbf{w}$  form the smallest unit parallelogram for

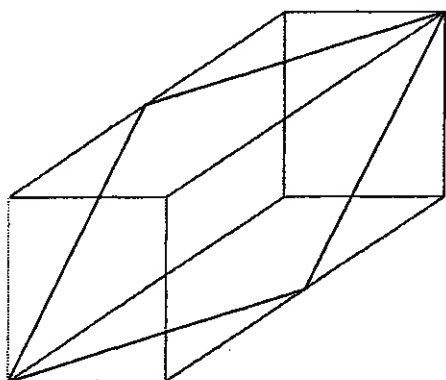


Figure 3: The unit brick of  $[111]$ , showing only the brick of unit cells (light lines) and the unit parallelogram (heavy lines). In this case there are  $h \times h \times (k + l) = 1 \times 1 \times 2 = 2$  unit cells per unit parallelogram of the plane  $[111]$ .

tessellating the plane  $hkl$  so that each parallelogram in the tessellation cuts bonds in the same pattern.

Corresponding to the unit parallelogram is a repeating set of unit cells, here called the repeating brick, of  $h \times h \times (k + l)$  unit cells, as illustrated in Figure 3 and Figure 4 in two different projections. In the repeating brick, the unit parallelogram intersects with  $h(h + k + l - 1)$  unit cells. It can be shown that this yields  $h$  copies each of  $h + k + l - 1$  different pieces. If we sum over different pieces to get  $n$  bonds, then overall they cut  $hn$  bonds. Since  $A_{hkl} = h\sqrt{h^2 + k^2 + l^2}$ , one has  $\sigma_{hkl} = n/\sqrt{h^2 + k^2 + l^2}$ . Thus it suffices to find the number of bonds cut by the  $h + k + l - 1$  different pieces. Now consider the projection of a unit cell onto the plane spanned by  $\hat{n}$  and  $\hat{k}$ . The plane  $[hkl]$  is projected onto a line and the unit cell onto a rectangle. The bonds appear as a network of lines. The position of the line corresponding to  $[hkl]$  is different in each of the different pieces. When the rectangle is rescaled to a unit square and all  $h + k + l - 1$  different cases are superimposed, we have a *calculation box*. For an example, consider Figure 5; in general the  $h + k + l - 1$  lines intersect the sides of the calculation box  $l$  times and the top and bottom  $h + k$  times.

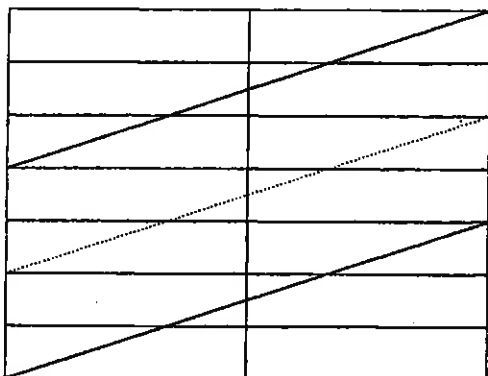


Figure 4: The unit brick of [234], projected onto the  $\hat{i}\hat{k}$  plane. Heavy lines show the unit parallelogram, and dotted lines its intersection of the planes  $z\hat{k} = 1, 2, \dots, h-1$ . Note that each of the two layers consists of 8 congruent pieces of the unit parallelogram. Each piece in one layer corresponds to a congruent piece in the other layer; such pairs have matching numbers.

In a calculation box, the line segments corresponding to the plane form a hatching with slope  $s = (h+k)/l$ . The intersections between the line segments of the plane and the line segments of the bonds give the count of bonds cut by the plane, as follows. If the plane  $[hkl]$  cuts a bond, then in the projection the bond will project onto a line segment partly above and partly below the plane. Conversely, if a bond is not cut by the plane it will project onto a line segment entirely on one side of the plane. In other words, the number of cut bonds is the number of intersections between the projection of the plane and the projections of the bonds. Where more than one bond projects onto a line segment, that segment obviously contributes more than one bond to the count.

The calculation is eased by one of two simple constructions. If the slope  $s < 1$ , the construction stacks two calculation boxes in a column. If  $s > 1$ , the construction lines up two calculation boxes in a row. In each construction the plane projects onto a set of line segments of equal length, as illustrated in Figure 6. These line segments we call *unit projections* of the cutting plane. When  $s < 1$ , there are  $l$  unit projections from left to right. When  $s > 1$  there are  $h+k$  unit projections from top to bottom.

We treat the case  $s < 1$  first. The  $l$  unit projections lie on the lines  $y_i = -sx + di + \delta$ , where  $d = 1/l$ ,  $i = 0, 1, \dots, l-1$  and  $\delta \in (0, d)$  is the offset. We define  $f(y_i)$  as the number of bonds cut by the unit projection that lies on line  $y_i$ . For  $i > k + h - l\delta$ , we have  $y_i(1) > 0$ , hence the

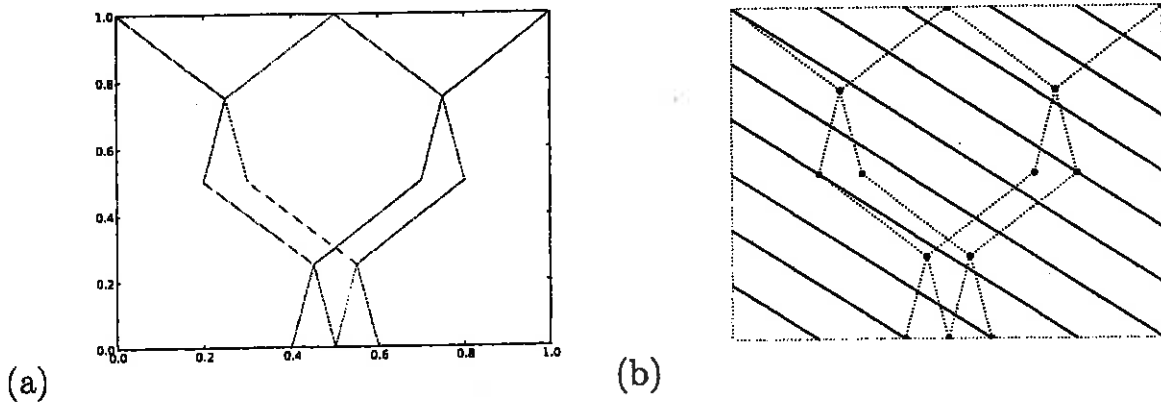


Figure 5:  
 (a) The calculation box of [236], with the plane suppressed, showing the position of the 16 bonds.  
 (b) The full superposition of the calculation box of [236]. The plane appears as 10 line segments.

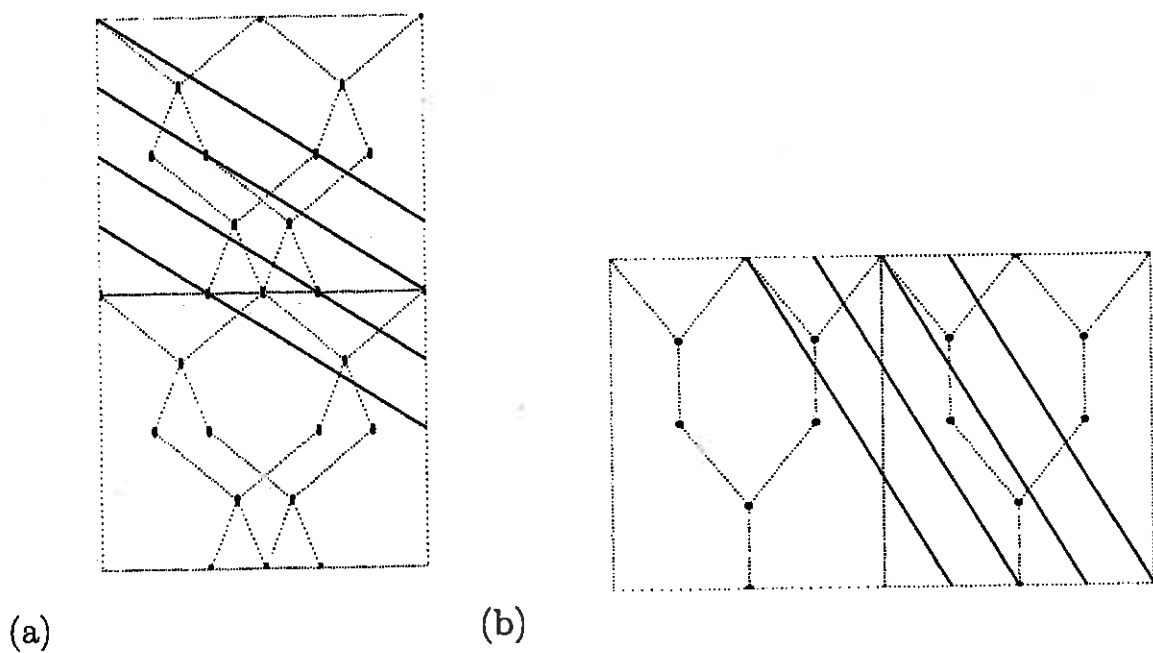


Figure 6: Examples of the construction of unit projections of the cutting plane. Bonds are dotted lines, atoms are discs, unit projections are solid lines.  
 (a) Case  $s < 1$ : there are  $l$  unit segments.  
 (b) Case  $s > 1$ : there are  $k + h$  unit segments.

line segments on those  $y_i$  go from right to left in one calculation box and therefore cut 4 bonds each. However, when  $i < k + h - l\delta$  we have  $y_i(\tilde{x}_i) = 0$  with  $\tilde{x}_i \in (0, 1)$  and the unit projections span two calculation boxes. On such  $y_i$  the unit projections cut either 3, 4 or 5 bonds. This is illustrated in Figure 6. The function  $f$  is therefore defined piecewise as follows:

$$f(y_i) = \begin{cases} 3 & \text{if } 0 < \tilde{x}_i < \frac{h}{h+k} \\ 4 & \text{if } \frac{h}{h+k} < \tilde{x}_i < \frac{k}{h+k} \\ 5 & \text{if } \frac{k}{h+k} < \tilde{x}_i < 1 \\ 4 & \text{otherwise,} \end{cases}$$

where  $i$ ,  $y_i$  and  $\tilde{x}_i$  are as defined above.

The number of bonds  $\#_{\{hkl\}}$  then is the minimum with respect to  $\delta$  of the sum of the  $f(y_i)$ :

$$\#_{\{hkl\}} = \min_{\delta} \sum_{i=0}^{l-1} f(y_i).$$

It is easily seen that  $f(y_i) = 3$  exactly as often as  $f(y_i) = 5$  for any  $d$ , and hence we have constant  $\#_{\{hkl\}} = 4l$ . Hence

$$\sigma_{hkl} = \frac{4l}{\sqrt{h^2 + k^2 + l^2}}, \quad (2)$$

for the case  $h + k < l$ .

One can define a similar function  $g(y_j)$  for the  $k + h$  line segments of the case  $k + h > l$ . For example, in the case  $hkl = 111$ , we have

$$f(y_i) = \begin{cases} 3 & \text{if } 0 < \tilde{x}_i < \frac{1}{8} \\ 1 & \text{if } \frac{1}{8} < \tilde{x}_i < \frac{1}{2} \\ 9 & \text{if } \frac{1}{2} < \tilde{x}_i < \frac{5}{8} \\ 3 & \text{if } \frac{5}{8} < \tilde{x}_i < 1 \end{cases}$$

From this it is easy to see that either 4 or 12 bonds are cut. The minimum is therefore 4 bonds, leading to  $\sigma_{111} = 4/\sqrt{3}$ . Curiously, this is the same as the value given by Equation 2. Also interesting is the average number of bonds cut when  $d$  ranges uniformly over  $(0, 0.5)$ . Since the case of 4 bonds is three times as frequent as the case of 12 bonds, the average is 6, which is also the value given by the Terentiev formula in Equation (3).

As this example shows, we have been able to treat  $s > 1$  only case by case, and have not found a general formula. Hence question A receives only a partial affirmative from us.



### 3 A probabilistic interpretation of Terentiev's formula

As noted above, Terentiev gives the formula:

$$\sigma_{\{111\}} = \sigma_{\{hkl\}} \sum_{i=1}^4 x_i \cos(\Phi_i) \quad (3)$$

for the surface energy of an arbitrary plane. Here  $x_i = \Phi_i / \sum_{j=1}^4 \Phi_j$ , and

$$\begin{aligned} \cos(\Phi_1) &= \frac{|h+k+l|}{\sqrt{3}\sqrt{h^2+k^2+l^2}}, \\ \cos(\Phi_2) &= \frac{|-h-k+l|}{\sqrt{3}\sqrt{h^2+k^2+l^2}}, \\ \cos(\Phi_3) &= \frac{|-h+k-l|}{\sqrt{3}\sqrt{h^2+k^2+l^2}}, \\ \cos(\Phi_4) &= \frac{|h-k-l|}{\sqrt{3}\sqrt{h^2+k^2+l^2}}. \end{aligned}$$

But since  $\sum_{i=1}^4 \cos^2(\Phi_i) = 4/3$ , an equivalent simpler form is

$$\sigma_{hkl} = \sigma_{111} \frac{3}{4} \sum_{i=1}^4 \cos(\Phi_i).$$

Then setting  $hkl = 111$  we reach the contradiction  $\sigma_{111} = 1.5\sigma_{111}$ .

So the Terentiev equation is not a general formula for  $\sigma_{hkl}$ . However, we note that the the vectors

$$\begin{aligned} \hat{\mathbf{a}} &= (\hat{\mathbf{i}} + \hat{\mathbf{j}} + \hat{\mathbf{k}})/\sqrt{3}, & \hat{\mathbf{b}} &= (-\hat{\mathbf{i}} - \hat{\mathbf{j}} + \hat{\mathbf{k}})/\sqrt{3}, \\ \hat{\mathbf{c}} &= (-\hat{\mathbf{i}} + \hat{\mathbf{j}} - \hat{\mathbf{k}})/\sqrt{3}, & \hat{\mathbf{d}} &= (\hat{\mathbf{i}} - \hat{\mathbf{j}} - \hat{\mathbf{k}})/\sqrt{3}, \end{aligned}$$

are the unit vectors giving the direction of the four bonds of an atom in the diamond lattice. Furthermore,  $\cos(\Phi_1) = \hat{\mathbf{a}} \cdot \mathbf{n}/|\mathbf{n}|$  gives the projection of one of the bonds onto the unit normal of the plane. One may interpret this as proportional to the probability of intersecting the bond in the direction of  $\hat{\mathbf{a}}$  by a random plane. The average overall number of bonds cut per unit area is then proportional to the sum:

$$\bar{\sigma}_{hkl} = C \sum_{i=1}^4 \cos(\Phi_i)$$

and setting  $hkl = 111$  we find that  $C = \bar{\sigma}_{111}/2$ . This gives

$$\bar{\sigma}_{hkl} = \bar{\sigma}_{111} \frac{1}{2} \sum_{i=1}^4 \cos(\Phi_i).$$

As we have seen, for  $h + k < l$  the average is equal to the minimum, so the Terentiev formula is exact for the same cases as ours. However, when  $h + k > l$  this is not always the case and then it is correct only in an average sense.

#### 4 Simulation of $\sigma_{hkl}$ versus temperature for a diamond in a melt

We repeat here the Terentiev simulation.

The unit-cell is a cube with edge length 3.569 Å, the length of a carbon bond is  $\sqrt{3}/4$  of the edge of the unit-cell, that is, 1.545 Å.

We place a number of (metal) molecules in a box where the bottom is the surface of the diamond. The potential energy consists of three terms.

- First we have the molecule - molecule interaction. The potential energy from a single pair of molecules with distance  $r$  is given by the Lennard-Jones potential

$$V_1(r) = a_1 r^{-12} - b_1 r^{-6}, \quad (4)$$

where  $a_1 = 24\,188.0647 \text{ eV } \text{Å}^{12}$  and  $b_1 = 201.4115 \text{ eV } \text{Å}^6$ .

- The molecules are kept in the box by the Lennard-Jones potential

$$V_2(r) = a_2 r^{-12} - b_2 r^{-6}, \quad (5)$$

where  $r$  is the distance to the boundary,  $a_2 = 7.4103 \text{ eV } \text{Å}^{12}$ , and  $b_2 = 2.68 \text{ eV } \text{Å}^6$ .

- Finally, the interaction with diamond lattice is modelled by the following "Lennard-Jones" potential for each atom-vacancy pair

$$V_3(r_0, r_1, r_2) = a_3 r_2^{-12} - b_3 (r_0 + r_1)^{-6}, \quad (6)$$

where  $r_0 = 1.545 \text{ Å}$  is the distance from the carbon atom to the vacant site,  $r_1$  is the distance from the molecule to the vacant site, and  $r_2$  is the distance from the molecule to the carbon atom,  $a_3 = 72.9949 \text{ eV } \text{Å}^{12}$ , and  $b_3 = 10.8808 \text{ eV } \text{Å}^6$ . This potential has a minimum at the vacant site and goes to infinity at the atom, as illustrated in Figure 7.

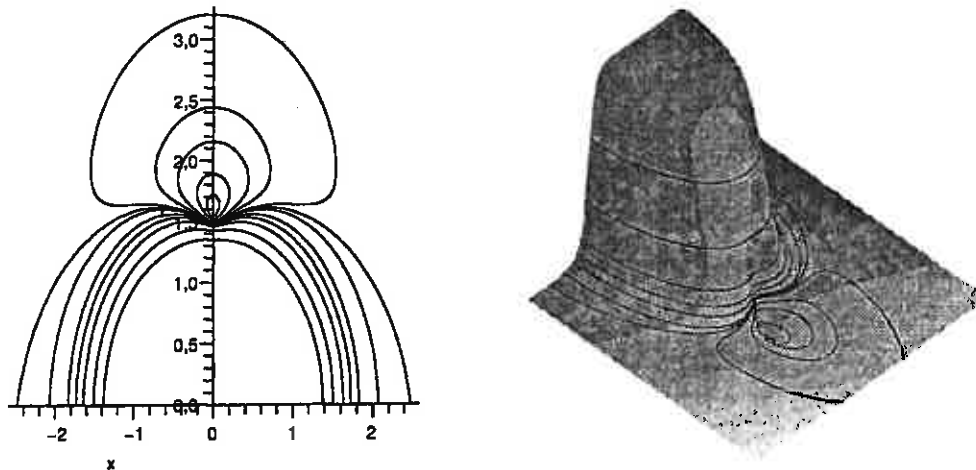


Figure 7: Contour lines for the  $V_3$  potential and a plot of  $\arctan(V_3)$ .

Using Matlab's optimisation toolbox we now minimise the potential energy and count the number of "free" vacant sites, where a site is considered free if the distance to any molecule is larger than  $1.3 \text{ \AA}$ .

Below we describe a general procedure which was used in the cases 111, 001 and 110.

First we look at the  $[001]$ -plane. It obviously cuts the unit cell in a square with side length 1, as illustrated in Figure 8. We use  $4 \times 4$  of this unit and let the height of the box be  $h$ . We parametrise the box with the unit cube  $[0, 1]^3$  as the domain in the following way

$$\begin{bmatrix} x \\ y \\ z \end{bmatrix} = \begin{bmatrix} 4 & 0 & 0 \\ 0 & 4 & 0 \\ 0 & 0 & h \end{bmatrix} \begin{bmatrix} u \\ v \\ w \end{bmatrix}, \quad (u, v, w) \in [0, 1]^3,$$

or in matrix notation  $\mathbf{x} = \mathbf{A}_{001}\mathbf{u}$ . The atom/vacant-site pairs have the

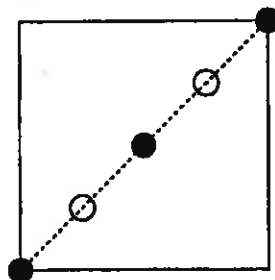


Figure 8: The intersection between the  $[001]$ -plane and the unit-cell. The side length is 1 and the area is 1. The atoms (filled) are all in the plane and the two "vacant sites" (open) are both  $1/4$  over the plane.

coordinates

$$\begin{bmatrix} x_a \\ y_a \\ z_a \end{bmatrix} = \begin{bmatrix} i \\ j \\ 0 \end{bmatrix}, \begin{bmatrix} 1/2 + i \\ 1/2 + j \\ 0 \end{bmatrix}, \begin{bmatrix} 1/2 + i \\ 1/2 + j \\ 0 \end{bmatrix}, \begin{bmatrix} 1 + i \\ 1 + j \\ 0 \end{bmatrix},$$

$$\begin{bmatrix} x_v \\ y_v \\ z_v \end{bmatrix} = \begin{bmatrix} 1/4 + i \\ 1/4 + j \\ 1/4 \end{bmatrix}, \begin{bmatrix} 1/4 + i \\ 1/4 + j \\ 1/4 \end{bmatrix}, \begin{bmatrix} 3/4 + i \\ 3/4 + j \\ 1/4 \end{bmatrix}, \begin{bmatrix} 3/4 + i \\ 3/4 + j \\ 1/4 \end{bmatrix},$$

where  $i, j = 0, 1, 2, 3$ . The corresponding  $(u, v, w)$  coordinates are

$$\mathbf{a} = \begin{bmatrix} u_a \\ v_a \\ w_a \end{bmatrix} = \begin{bmatrix} i/4 \\ j/4 \\ 0 \end{bmatrix}, \begin{bmatrix} 1/8 + i/4 \\ 1/8 + j/4 \\ 0 \end{bmatrix}, \begin{bmatrix} 1/8 + i/4 \\ 1/8 + j/4 \\ 0 \end{bmatrix}, \begin{bmatrix} 1/4 + i/4 \\ 1/4 + j/4 \\ 0 \end{bmatrix},$$

$$\mathbf{v} = \begin{bmatrix} u_v \\ v_v \\ w_v \end{bmatrix} = \begin{bmatrix} 1/16 + i/4 \\ 1/16 + j/4 \\ 1/(4h) \end{bmatrix}, \begin{bmatrix} 1/16 + i/4 \\ 1/16 + j/4 \\ 1/(4h) \end{bmatrix}, \begin{bmatrix} 3/16 + i/4 \\ 3/16 + j/4 \\ 1/(4h) \end{bmatrix}, \begin{bmatrix} 3/16 + i/4 \\ 3/16 + j/4 \\ 1/(4h) \end{bmatrix}.$$

The length of a vector  $\mathbf{u}$  in  $(u, v, w)$  coordinates is given by

$$\|\mathbf{u}\|^2 = \mathbf{u}^T \mathbf{A}_{001}^T \mathbf{A}_{001} \mathbf{u} = [u \ v \ w] \begin{bmatrix} 16 & 0 & 0 \\ 0 & 16 & 0 \\ 0 & 0 & h^2 \end{bmatrix} \begin{bmatrix} u \\ v \\ w \end{bmatrix}$$

and the distance between two points corresponding to the coordinates  $\mathbf{u}, \mathbf{v} \in [0, 1]^3$  is  $\|\mathbf{u} - \mathbf{v}\|$ . Consider a point with coordinates  $(u, v, w) \in [0, 1]^3$ . Then the distance to the floor and to the roof is  $hw$  and  $h(1 - w)$  respectively, the distance to the sides  $u = 0$  and  $u = 1$  is  $4u$  and  $4(1 - u)$  respectively, and the distance to the sides  $v = 0$  and  $v = 1$  is  $4v$  and  $4(1 - v)$  respectively. Now it is possible to write the potential energy,  $v$ , in  $(u, v, w)$  coordinates:

$$\begin{aligned}
V &= \sum_{i < j} (a_1 \|\mathbf{u}_i - \mathbf{u}_j\|^{-12} - b_1 \|\mathbf{u}_i - \mathbf{u}_j\|^{-6}) \\
&+ \sum_i (a_2 (4u_i)^{-12} - b_2 (4u_i)^{-6} + a_2 (4(1 - u_i))^{-12} - b_2 (4(1 - u_i))^{-6}) \\
&+ \sum_i (a_2 (4v_i)^{-12} - b_2 (4v_i)^{-6} + a_2 (4(1 - v_i))^{-12} - b_2 (4(1 - v_i))^{-6}) \\
&+ \sum_i (a_2 (hw_i)^{-12} - b_2 (hw_i)^{-6} + a_2 (h(1 - w_i))^{-12} - b_2 (h(1 - w_i))^{-6}) \\
&+ \sum_j \sum_i (a_3 \|\mathbf{u}_i - \mathbf{a}_j\|^{-12} - b_3 (\|\mathbf{a}_j - \mathbf{v}_j\| + \|\mathbf{u}_i - \mathbf{v}_j\|)^{-6}) \\
&= \sum_{i < j} \left( a_1 ((\mathbf{u}_i - \mathbf{u}_j)^T \mathbf{A}_{001}^T \mathbf{A}_{001} (\mathbf{u}_i - \mathbf{u}_j))^{-6} \right. \\
&\quad \left. - b_1 ((\mathbf{u}_i - \mathbf{u}_j)^T \mathbf{A}_{001}^T \mathbf{A}_{001} (\mathbf{u}_i - \mathbf{u}_j))^{-3} \right) \\
&+ \sum_i (a_2 (4u_i)^{-12} - b_2 (4u_i)^{-6} + a_2 (4(1 - u_i))^{-12} - b_2 (4(1 - u_i))^{-6}) \\
&+ \sum_i (a_2 (4v_i)^{-12} - b_2 (4v_i)^{-6} + a_2 (4(1 - v_i))^{-12} - b_2 (4(1 - v_i))^{-6}) \\
&+ \sum_i (a_2 (hw_i)^{-12} - b_2 (hw_i)^{-6} + a_2 (h(1 - w_i))^{-12} - b_2 (h(1 - w_i))^{-6}) \\
&+ \sum_j \sum_i \left( a_3 ((\mathbf{u}_i - \mathbf{a}_j)^T \mathbf{A}_{001}^T \mathbf{A}_{001} (\mathbf{u}_i - \mathbf{a}_j))^{-6} \right. \\
&\quad \left. - b_3 \left( d + \sqrt{(\mathbf{u}_i - \mathbf{v}_j)^T \mathbf{A}_{001}^T \mathbf{A}_{001} (\mathbf{u}_i - \mathbf{v}_j)} \right)^{-6} \right),
\end{aligned}$$

where  $\mathbf{u}_i = (u_i, v_i, w_i)$  are the coordinates for the molecules,  $\mathbf{a}_j = (u_{a,j}, v_{a,j}, w_{a,j})$  are the coordinates for the carbon atoms,  $\mathbf{v}_j = (u_{v,j}, v_{v,j}, w_{v,j})$  are the coordinates for the vacant sites, and  $d = \sqrt{3}/4$  is the (constant) distance between two neighbouring atoms in the diamond lattice.

The [110]-plane cuts the unit cell in a rectangle with side lengths 1 and  $\sqrt{2}$ , as shown in Figure 9. We use  $3 \times 4$  of this unit and as before let  $h$  denote the height of the box. We parametrise the box with the unit cube

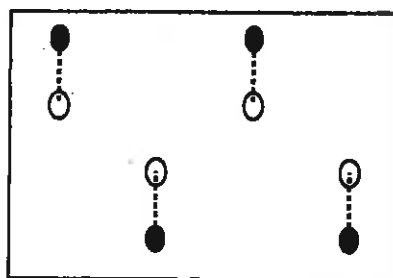


Figure 9: The intersection between the  $[110]$ -plane and the unit-cell. The side lengths are 1 and  $\sqrt{2}$  and the area is  $\sqrt{2}$ . The atoms (filled) are all in the plane and the "vacant sites" (open) are all  $\sqrt{2}/4$  over the plane.

$[0, 1]^3$  as the domain in the following way:

$$\begin{bmatrix} x \\ y \\ z \end{bmatrix} = \begin{bmatrix} 3\sqrt{2} & 0 & 0 \\ 0 & 4 & 0 \\ 0 & 0 & h \end{bmatrix} \begin{bmatrix} u \\ v \\ w \end{bmatrix}, \quad (u, v, w) \in [0, 1]^3,$$

or, in matrix notation,  $\mathbf{x} = \mathbf{A}_{110}\mathbf{u}$ . The atom/vacant-site pairs have the coordinates

$$\begin{bmatrix} x_a \\ y_a \\ z_a \end{bmatrix} = \begin{bmatrix} 3\sqrt{2}/8 + i\sqrt{2} \\ 1/8 + j \\ 0 \end{bmatrix}, \begin{bmatrix} 7\sqrt{2}/8 + i\sqrt{2} \\ 1/8 + j \\ 0 \end{bmatrix}, \begin{bmatrix} \sqrt{2}/8 + i\sqrt{2} \\ 7/8 + j \\ 0 \end{bmatrix}, \begin{bmatrix} 5\sqrt{2}/8 + i\sqrt{2} \\ 7/8 + j \\ 0 \end{bmatrix},$$

$$\begin{bmatrix} x_v \\ y_v \\ z_v \end{bmatrix} = \begin{bmatrix} 3\sqrt{2}/8 + i\sqrt{2} \\ 3/8 + j \\ 1/4 \end{bmatrix}, \begin{bmatrix} 7\sqrt{2}/8 + i\sqrt{2} \\ 3/8 + j \\ 1/4 \end{bmatrix}, \begin{bmatrix} \sqrt{2}/8 + i\sqrt{2} \\ 5/8 + j \\ 1/4 \end{bmatrix}, \begin{bmatrix} 5\sqrt{2}/8 + i\sqrt{2} \\ 5/8 + j \\ 1/4 \end{bmatrix},$$

where  $i = 0, 1, 2$  and  $j = 0, 1, 2, 3$ . The corresponding  $(u, v, w)$  coordinates are

$$\mathbf{a} = \begin{bmatrix} u_a \\ v_a \\ w_a \end{bmatrix} = \begin{bmatrix} 3/24 + i/3 \\ 1/32 + j/4 \\ 0 \end{bmatrix}, \begin{bmatrix} 7/24 + i/3 \\ 1/32 + j/4 \\ 0 \end{bmatrix}, \begin{bmatrix} 1/24 + i/3 \\ 7/32 + j/4 \\ 0 \end{bmatrix}, \begin{bmatrix} 5/24 + i/3 \\ 7/32 + j/4 \\ 0 \end{bmatrix},$$

$$\mathbf{v} = \begin{bmatrix} u_v \\ v_v \\ w_v \end{bmatrix} = \begin{bmatrix} 3/24 + i/3 \\ 3/32 + j/4 \\ 1/(4h) \end{bmatrix}, \begin{bmatrix} 7/24 + i/3 \\ 3/32 + j/4 \\ 1/(4h) \end{bmatrix}, \begin{bmatrix} 1/24 + i/3 \\ 5/32 + j/4 \\ 1/(4h) \end{bmatrix}, \begin{bmatrix} 5/24 + i/3 \\ 5/32 + j/4 \\ 1/(4h) \end{bmatrix}.$$

The length of a vector  $\mathbf{u}$  in  $(u, v, w)$  coordinates is given by

$$\|\mathbf{u}\|^2 = \mathbf{u}^T \mathbf{A}_{110}^T \mathbf{A}_{110} \mathbf{u} = [u \ v \ w] \begin{bmatrix} 18 & 0 & 0 \\ 0 & 16 & 0 \\ 0 & 0 & h^2 \end{bmatrix} \begin{bmatrix} u \\ v \\ w \end{bmatrix}$$

and the distance between two points corresponding to the coordinates  $\mathbf{u}, \mathbf{v} \in [0, 1]^3$  is  $\|\mathbf{u} - \mathbf{v}\|$ . Consider a point with coordinates  $(u, v, w) \in [0, 1]^3$ . Then the distance to the floor and to the roof is still  $hw$  and  $h(1-w)$  respectively. The  $(x, y)$  coordinates of the point are  $((6u+3v)\sqrt{2}/2, 3v\sqrt{6}/2)$  so the distance to sides  $v = 0$  and  $v = 1$  is  $v3\sqrt{6}/2$  and  $(1-v)3\sqrt{6}/2$  respectively. Finally, the sides  $u = 0$  and  $u = 1$  corresponds to the lines  $t(1, \sqrt{3})$  and  $(3\sqrt{2}, 0) + t(1, \sqrt{3})$  respectively. The signed distances to these lines are

$$\frac{\sqrt{3}x - y}{2} = \frac{\sqrt{3}(6u + 3v)\sqrt{2} - 3v\sqrt{6}}{4} = \frac{3\sqrt{6}}{2}u$$

and

$$\frac{-\sqrt{3}(x - 3\sqrt{2}) + y}{2} = \frac{3\sqrt{6}}{2}(1 - u),$$

respectively. This is of course obvious from symmetry. Now it is possible to write the potential energy,  $V$ , in  $(u, v, w)$  coordinates:

$$\begin{aligned}
V &= \sum_{i < j} (a_1 \|\mathbf{u}_i - \mathbf{u}_j\|^{-12} - b_1 \|\mathbf{u}_i - \mathbf{u}_j\|^{-6}) \\
&+ \sum_i \left( a_2 \left( \frac{3\sqrt{6}}{2} u_i \right)^{-12} - b_2 \left( \frac{3\sqrt{6}}{2} u_i \right)^{-6} + a_2 \left( \frac{3\sqrt{6}}{2} (1 - u_i) \right)^{-12} - b_2 \left( \frac{3\sqrt{6}}{2} (1 - u_i) \right)^{-6} \right) \\
&+ \sum_i \left( a_2 \left( \frac{3\sqrt{6}}{2} v_i \right)^{-12} - b_2 \left( \frac{3\sqrt{6}}{2} v_i \right)^{-6} + a_2 \left( \frac{3\sqrt{6}}{2} (1 - v_i) \right)^{-12} - b_2 \left( \frac{3\sqrt{6}}{2} (1 - v_i) \right)^{-6} \right) \\
&+ \sum_i (a_2 (hw_i)^{-12} - b_2 (hw_i)^{-6} + a_2 (h(1 - w_i))^{-12} - b_2 (h(1 - w_i))^{-6}) \\
&+ \sum_j \sum_i (a_3 \|\mathbf{u}_i - \mathbf{a}_j\|^{-12} - b_3 (\|\mathbf{a}_j - \mathbf{v}_j\| + \|\mathbf{u}_i - \mathbf{v}_j\|)^{-6}) \\
&= \sum_{i < j} \left( a_1 \left( (\mathbf{u}_i - \mathbf{u}_j)^T \mathbf{A}_{111}^T \mathbf{A}_{111} (\mathbf{u}_i - \mathbf{u}_j) \right)^{-6} - b_1 \left( (\mathbf{u}_i - \mathbf{u}_j)^T \mathbf{A}_{111}^T \mathbf{A}_{111} (\mathbf{u}_i - \mathbf{u}_j) \right)^{-3} \right) \\
&+ \sum_i \left( a_2 \left( \frac{3\sqrt{6}}{2} u_i \right)^{-12} - b_2 \left( \frac{3\sqrt{6}}{2} u_i \right)^{-6} + a_2 \left( \frac{3\sqrt{6}}{2} (1 - u_i) \right)^{-12} - b_2 \left( \frac{3\sqrt{6}}{2} (1 - u_i) \right)^{-6} \right) \\
&+ \sum_i \left( a_2 \left( \frac{3\sqrt{6}}{2} v_i \right)^{-12} - b_2 \left( \frac{3\sqrt{6}}{2} v_i \right)^{-6} + a_2 \left( \frac{3\sqrt{6}}{2} (1 - v_i) \right)^{-12} - b_2 \left( \frac{3\sqrt{6}}{2} (1 - v_i) \right)^{-6} \right) \\
&+ \sum_i (a_2 (hw_i)^{-12} - b_2 (hw_i)^{-6} + a_2 (h(1 - w_i))^{-12} - b_2 (h(1 - w_i))^{-6}) \\
&+ \sum_j \sum_i \left( a_3 \left( (\mathbf{u}_i - \mathbf{a}_j)^T \mathbf{A}_{111}^T \mathbf{A}_{111} (\mathbf{u}_i - \mathbf{a}_j) \right)^{-6} \right. \\
&\quad \left. - b_3 \left( d + \sqrt{(\mathbf{u}_i - \mathbf{v}_j)^T \mathbf{A}_{111}^T \mathbf{A}_{111} (\mathbf{u}_i - \mathbf{v}_j)} \right)^{-6} \right),
\end{aligned}$$

where  $\mathbf{u}_i = (u_i, v_i, w_i)$  are the coordinates for the molecules,  $\mathbf{a}_j = (u_{a,j}, v_{a,j}, w_{a,j})$  are the coordinates for the carbon atoms,  $\mathbf{v}_j = (u_{v,j}, v_{v,j}, w_{v,j})$  are the coordinates for the vacant sites, and  $d = \sqrt{3}/4$  is the (constant) distance between two neighbouring atoms in the diamond lattice.

The [111]-plane cuts two unit cells in a parallelogram spanned by the vectors  $(\sqrt{2}, 0)$  and  $(\sqrt{2}/2, \sqrt{6}/2)$  as in Figure 10. We use  $3 \times 3$  of this unit and as before let  $h$  denote the height of the box. We parametrise the box with the unit cube  $[0, 1]^3$  as the domain in the following way:

$$\begin{bmatrix} x \\ y \\ z \end{bmatrix} = \begin{bmatrix} 3\sqrt{2} & 3\sqrt{2}/2 & 0 \\ 0 & 3\sqrt{6}/2 & 0 \\ 0 & 0 & h \end{bmatrix} \begin{bmatrix} u \\ v \\ w \end{bmatrix}, \quad (u, v, w) \in [0, 1]^3,$$



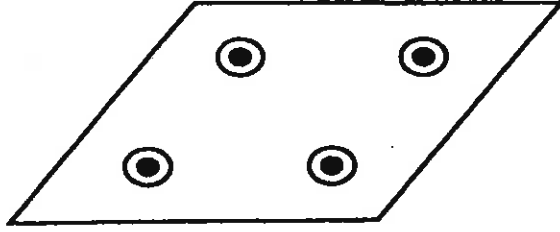


Figure 10: The intersection between the [111]-plane and two unit-cells is a parallelogram spanned by  $(\sqrt{2}, 0)$  and  $(\sqrt{2}/2, \sqrt{6}/2)$ . The side length is  $\sqrt{2}$  and the area is  $\sqrt{3}$ . The atoms (filled) are all in the plane and the "vacant sites" (open) are all  $\sqrt{3}/4$  over the plane, and with a bond to the atom below.

or, in matrix notation,  $\mathbf{x} = \mathbf{A}_{111}\mathbf{u}$ . The atom/vacant-site pairs have the coordinates

$$\begin{bmatrix} x_a \\ y_a \\ z_a \end{bmatrix} = \begin{bmatrix} 3\sqrt{2}/8 + (2i + j)\sqrt{2}/2 \\ \sqrt{6}/8 + j\sqrt{2}/2 \\ 0 \end{bmatrix}, \begin{bmatrix} 7\sqrt{2}/8 + (2i + j)\sqrt{2}/2 \\ \sqrt{6}/8 + j\sqrt{2}/2 \\ 0 \end{bmatrix}, \\ \begin{bmatrix} 5\sqrt{2}/8 + (2i + j)\sqrt{2}/2 \\ 3\sqrt{6}/8 + j\sqrt{2}/2 \\ 0 \end{bmatrix}, \begin{bmatrix} 9\sqrt{2}/8 + (2i + j)\sqrt{2}/2 \\ 3\sqrt{6}/8 + j\sqrt{2}/2 \\ 0 \end{bmatrix},$$

$$\begin{bmatrix} x_v \\ y_v \\ z_v \end{bmatrix} = \begin{bmatrix} 3\sqrt{2}/8 + (2i + j)\sqrt{2}/2 \\ \sqrt{6}/8 + j\sqrt{2}/2 \\ \sqrt{3}/4 \end{bmatrix}, \begin{bmatrix} 7\sqrt{2}/8 + (2i + j)\sqrt{2}/2 \\ \sqrt{6}/8 + j\sqrt{2}/2 \\ \sqrt{3}/4 \end{bmatrix}, \\ \begin{bmatrix} 5\sqrt{2}/8 + (2i + j)\sqrt{2}/2 \\ 3\sqrt{6}/8 + j\sqrt{2}/2 \\ \sqrt{3}/4 \end{bmatrix}, \begin{bmatrix} 9\sqrt{2}/8 + (2i + j)\sqrt{2}/2 \\ 3\sqrt{6}/8 + j\sqrt{2}/2 \\ \sqrt{3}/4 \end{bmatrix},$$

where  $i = 0, 1, 2$  and  $j = 0, 1, 2$ . The corresponding  $(u, v, w)$  coordinates are

$$\mathbf{a} = \begin{bmatrix} u_a \\ v_a \\ w_a \end{bmatrix} = \begin{bmatrix} 1/12 + i/3 \\ 1/12 + j/3 \\ 0 \end{bmatrix}, \begin{bmatrix} 3/12 + i/3 \\ 1/12 + j/3 \\ 0 \end{bmatrix}, \begin{bmatrix} 1/12 + i/3 \\ 3/12 + j/3 \\ 0 \end{bmatrix}, \begin{bmatrix} 3/12 + i/3 \\ 3/12 + j/3 \\ 0 \end{bmatrix},$$

$$\mathbf{v} = \begin{bmatrix} u_v \\ v_v \\ w_v \end{bmatrix} = \begin{bmatrix} 1/12 + i/3 \\ 1/12 + j/3 \\ \sqrt{3}/(4h) \end{bmatrix}, \begin{bmatrix} 3/12 + i/3 \\ 1/12 + j/3 \\ \sqrt{3}/(4h) \end{bmatrix}, \begin{bmatrix} 1/12 + i/3 \\ 3/12 + j/3 \\ \sqrt{3}/(4h) \end{bmatrix}, \begin{bmatrix} 3/12 + i/3 \\ 3/12 + j/3 \\ \sqrt{3}/(4h) \end{bmatrix}.$$

The length of a vector  $\mathbf{u}$  in  $(u, v, w)$  coordinates is given by

$$\|\mathbf{u}\|^2 = \mathbf{u}^T \mathbf{A}_{111}^T \mathbf{A}_{111} \mathbf{u} = [u \quad v \quad w] \begin{bmatrix} 18 & 9 & 0 \\ 9 & 18 & 0 \\ 0 & 0 & h^2 \end{bmatrix} \begin{bmatrix} u \\ v \\ w \end{bmatrix}$$

and the distance between two points corresponding to the coordinates  $\mathbf{u}, \mathbf{v} \in [0, 1]^3$  is  $\|\mathbf{u} - \mathbf{v}\|$ . Consider a point with coordinates  $(u, v, w) \in [0, 1]^3$ . Then the distance to the floor and to the roof is still  $hw$  and  $h(1-w)$  respectively. The  $(x, y)$  coordinates of the point are  $((6u+3v)\sqrt{2}/2, 3v\sqrt{6}/2)$  so the distance to sides  $v = 0$  and  $v = 1$  is  $v3\sqrt{6}/2$  and  $(1-v)3\sqrt{6}/2$  respectively. Finally, the sides  $u = 0$  and  $u = 1$  corresponds to the lines  $t(1, \sqrt{3})$  and  $(3\sqrt{2}, 0) + t(1, \sqrt{3})$  respectively. The signed distances to these lines are

$$\frac{\sqrt{3}x - y}{2} = \frac{\sqrt{3}(6u + 3v)\sqrt{2} - 3v\sqrt{6}}{4} = \frac{3\sqrt{6}}{2}u$$

and

$$\frac{-\sqrt{3}(x - 3\sqrt{2}) + y}{2} = \frac{3\sqrt{6}}{2}(1 - u),$$

respectively. This is of course obvious from symmetry. Now it is possible to write the potential energy,  $V$ , in  $(u, v, w)$  coordinates:

$$\begin{aligned}
V &= \sum_{i < j} (a_1 \|\mathbf{u}_i - \mathbf{u}_j\|^{-12} - b_1 \|\mathbf{u}_i - \mathbf{u}_j\|^{-6}) \\
&+ \sum_i \left( a_2 \left( \frac{3\sqrt{6}}{2} u_i \right)^{-12} - b_2 \left( \frac{3\sqrt{6}}{2} u_i \right)^{-6} + a_2 \left( \frac{3\sqrt{6}}{2} (1 - u_i) \right)^{-12} - b_2 \left( \frac{3\sqrt{6}}{2} (1 - u_i) \right)^{-6} \right) \\
&+ \sum_i \left( a_2 \left( \frac{3\sqrt{6}}{2} v_i \right)^{-12} - b_2 \left( \frac{3\sqrt{6}}{2} v_i \right)^{-6} + a_2 \left( \frac{3\sqrt{6}}{2} (1 - v_i) \right)^{-12} - b_2 \left( \frac{3\sqrt{6}}{2} (1 - v_i) \right)^{-6} \right) \\
&+ \sum_i (a_2 (hw_i)^{-12} - b_2 (hw_i)^{-6} + a_2 (h(1 - w_i))^{-12} - b_2 (h(1 - w_i))^{-6}) \\
&+ \sum_j \sum_i (a_3 \|\mathbf{u}_i - \mathbf{a}_j\|^{-12} - b_3 (\|\mathbf{a}_j - \mathbf{v}_j\| + \|\mathbf{u}_i - \mathbf{v}_j\|)^{-6}) \\
&= \sum_{i < j} \left( a_1 \left( (\mathbf{u}_i - \mathbf{u}_j)^T \mathbf{A}_{111}^T \mathbf{A}_{111} (\mathbf{u}_i - \mathbf{u}_j) \right)^{-6} - b_1 \left( (\mathbf{u}_i - \mathbf{u}_j)^T \mathbf{A}_{111}^T \mathbf{A}_{111} (\mathbf{u}_i - \mathbf{u}_j) \right)^{-3} \right) \\
&+ \sum_i \left( a_2 \left( \frac{3\sqrt{6}}{2} u_i \right)^{-12} - b_2 \left( \frac{3\sqrt{6}}{2} u_i \right)^{-6} + a_2 \left( \frac{3\sqrt{6}}{2} (1 - u_i) \right)^{-12} - b_2 \left( \frac{3\sqrt{6}}{2} (1 - u_i) \right)^{-6} \right) \\
&+ \sum_i \left( a_2 \left( \frac{3\sqrt{6}}{2} v_i \right)^{-12} - b_2 \left( \frac{3\sqrt{6}}{2} v_i \right)^{-6} + a_2 \left( \frac{3\sqrt{6}}{2} (1 - v_i) \right)^{-12} - b_2 \left( \frac{3\sqrt{6}}{2} (1 - v_i) \right)^{-6} \right) \\
&+ \sum_i (a_2 (hw_i)^{-12} - b_2 (hw_i)^{-6} + a_2 (h(1 - w_i))^{-12} - b_2 (h(1 - w_i))^{-6}) \\
&+ \sum_j \sum_i \left( a_3 \left( (\mathbf{u}_i - \mathbf{a}_j)^T \mathbf{A}_{111}^T \mathbf{A}_{111} (\mathbf{u}_i - \mathbf{a}_j) \right)^{-6} \right. \\
&\quad \left. - b_3 \left( d + \sqrt{(\mathbf{u}_i - \mathbf{v}_j)^T \mathbf{A}_{111}^T \mathbf{A}_{111} (\mathbf{u}_i - \mathbf{v}_j)} \right)^{-6} \right),
\end{aligned}$$

where  $\mathbf{u}_i = (u_i, v_i, w_i)$  are the coordinates for the molecules,  $\mathbf{a}_j = (u_{a,j}, v_{a,j}, w_{a,j})$  are the coordinates for the carbon atoms,  $\mathbf{v}_j = (u_{v,j}, v_{v,j}, w_{v,j})$  are the coordinates for the vacant sites, and  $d = \sqrt{3}/4$  is the (constant) distance between two neighbouring atoms in the diamond lattice.

#### 4.1 Results

We have not attempted to replicate exactly the diagram in Terentiev. This is for two reasons. Firstly, the degree of smoothness in his diagram would require a much larger computation than the one described above. Secondly, we are unable to present results in terms of temperature. In the paper by Terentiev [1], the point is made that low density corresponds to high temperature. The claim is made that they are inversely proportional. We have not attempted to prove this claim or to find the constant of proportionality.

Hence we present our simulation results in terms of inversed density.

With these provisos, we show in Figure 11 typical results of running this algorithm. The high-temperature behaviour is correct, in that the surface energy of the 111-plane is the lowest, and that of the 100-plane is the highest. At low temperatures the resolution is poor, and the results cannot be said to be definitive. However, they are encouraging, in that the surface energy of the 111-plane appears to be approaching 0 more slowly with decreasing "temperature" than that of the 110-plane, which itself appears to go more slowly than that of the 100-plane. We believe large-scale implementations of the algorithm above would have better resolution, and in all likelihood the diagram of Terentiev [1] would be replicated.

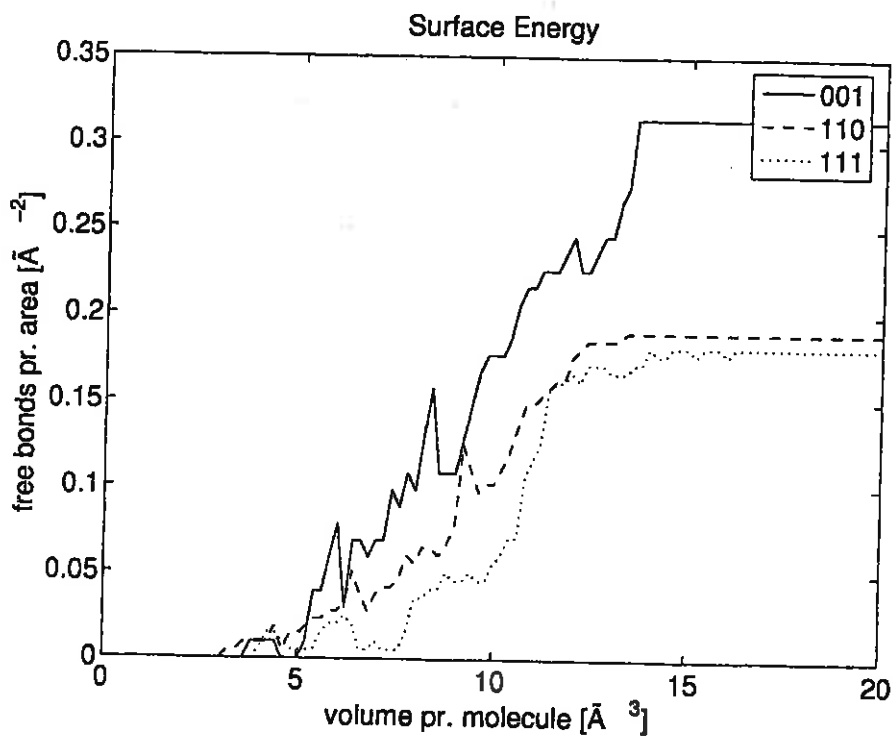


Figure 11: Simulation results: the surface energy, in terms of bonds per unit area, as a function of the inverse molecular density (as proxy for temperature). Simulations boxes have a basis intersecting 12 to 16 unit cells and contain 200 atoms of melt.

## 5 Further work

Obviously one would like to have a general formula for the vacuum surface energy also for the case  $s > 1$ . In that case, as we have seen, the value of  $f(y_i)$  changes at many places. It is easy to see that these are projections of the atoms that appear internal to the calculation box. The order in which these projections line up on the bottom plane is not constant, but depends on  $h, k$ , and  $l$ . It should be investigated whether the number of different possible orders are manageably small. If so, it may be that the bond count leading to  $f(y_i)$  may be tractable.

## References

- [1] Terentiev, S. Molecular-dynamics simulation of the effect of temperature of the growth environment on diamond habit. *Diamond and Related Materials*, 8 (1999), 1444–1450.
- [2] Blank, V. D., Kuznetsov, M. S., Nosukhin, S. A., Terentiev, S. A. and Denisov, V. N. The influence of crystallization temperature and boron concentration in growth environment on its distribution in growth sectors of type IIb diamond. *Diamond and Related Materials*, 16 (2007), 800–804.
- [3] Lee, B. J. and Lee, L. W. A modified embedded atom method in interatomic potential for carbon. *Calphad-Computer Coupling of Phase Diagrams and Thermochemistry*. 29 (2005), 7–16.
- [4] Titkov, S. V., Saporin, G. V. and Obyden, S. K. Evolution of growth sectors in natural diamond crystals as revealed by cathodoluminescence topography. *Geology of Ore Deposits*, 44 (2002), 350–360.
- [5] Zhang, J.-M., Ma, F., Xu, K.-W. and Xin, X.-X. Anisotropy analysis of the surface energy of diamond cubic crystals. *Surface and Interface Analysis*, 8 (2003), 805–809.